Experimental study of multiquantum, multiphoton resonances and Bloch-Siegert shifts in low-frequency EPR spectra

Ilmas Sadykov

Kazan Federal University, 420008, Kazan, Russia

Annotation.   The EPR from the DPPG was investigated on a spectrometer with different angles between a constant polarization field and an adjustable RF pump field at a frequency of 20 MHz in a continuous mode and a receiver tuned to the second harmonic frequency of the EPR signal. A technique for processing and more accurate measurement of the parameters of the EPR lines and the Bloch – Siegert shift is proposed. The conditions for maximizing the signal of even EPR harmonics are obtained depending on the angle of inclination of the HF field to the constant field. On the basis of experimental data and numerical solutions of the Bloch system of differential equations, the effect of asymmetry and a change in the sign of the second harmonic of the EPR line when the direction of the constant field is reversed is discovered and explained. An additional effect of displacement of the resonance line was discovered due to the inhomogeneous polarization of this line during scanning of the polarizing field. The effect of the appearance of the observed and possible resonant EPR harmonics is explained by the frequency modulation of the resonance conditions by both the perpendicular and parallel components of the RF pump field. It is concluded that the Bloch equations describe well in quality and satisfactory in accuracy all the observed parameters of EPR lines, such as intensity, width, shape, and their shifts. It is also shown that these equations describe the experiment on Bloch-Siegert shifts at least five times more accurately than the data of competing theories. A detailed description of the spectrometer is given and a computer program for the numerical calculation of the EPR spectra is presented.
       E-mail: ilmas-im-sadykov@yandex.ru

Introduction

Historically, by analogy with quantum optics [1], forbidden magnetic dipole transitions in electron paramagnetic resonance (EPR) began to be called multiquantum [2], [3, p. 146]. For the first time, such forbidden EPR lines were observed by E.K. Zavoisky. on manganese salts with spin S = ± 5⁄2 [4]. In his experiment, resonance lines were observed in fields two, three, four and five times smaller than the field of the main resonance (transitions with a change in the magnetic quantum number ΔM = ± 1) at a fixed generator frequency (3.54 GHz). However, there were no such resonances, except for the main one, from copper ions with spin S = ± 1⁄2. Similar results were obtained in [5, p.577] at a frequency of 16.1 GHz on cobalt ions (S = ± 1⁄2), which contradicted the theoretical calculations of E.K. Zavoisky. Moreover, one line was observed at a field half of the main resonance with a signal amplitude ~ 160 times smaller than the line of the main EPR. There are also more modern works devoted to the detection of forbidden two-quantum EPR transitions in magnetic nanoparticles [6], [7].

In all the above theoretical and experimental studies, the frequency of action of an alternating field (pumping) on the spin system and the frequency of its response were equal, and resonances arose in fractional fields relative to the field of the main resonance. It is believed that at a low pump intensity, one-photon processes occur with absorption and emission of one photon [8].

With an increase in the pump intensity (number of photons), EPR signals appear at frequencies that are multiples of the pump frequency. For example, in [9], the behavior of the second harmonic of the reemission of the pump energy by a spin system from DPPH and ruby was studied experimentally and theoretically at the temperature of liquid helium. In this case, the pump power per pulse could reach one kilowatt.

In our work [10], we also studied a relatively low-frequency (11 MHz) EPR from DPPG in a continuous mode with a wide range of the RF pumping level at room temperature, where not only the second harmonic of the EPR signal, but also the third harmonic were detected. Moreover, these harmonics arose not only at the fields of the fundamental (main) resonance, corresponding to transitions with $\Delta M = \pm 1$, but also at fields three times higher than the fundamental one. Such effects are explained in the literature by multiphoton processes [11], [12]. If the EPR spectrometers use sufficiently intense perpendicular alternating fields to a constant field in a continuous mode, then a shift of the resonance lines towards lower constant fields occurs. The possibility of the appearance of such a concomitant effect in magnetic resonance was theoretically predicted by F. Bloch and A. Siegert (BS) [13]. Such effects arise not only in EPR and NMR, but also in a wider spectrum of phenomena of atomic radio spectroscopy [14]. In order to avoid confusion in terminology [12], [15], in what follows in our text we will use names that better reflect the essence of the experimental results - fractional-field (instead of multi-quantum), multi-field and multi-frequency (instead of multi-photon) relative to the field and frequency of the main resonance. Then, following work [10], this article will use the indices **m** and **n** to denote the multiplicities of fields and frequencies, respectively. Resonances corresponding to these indices will be written as R{m,n}. Thus, the traditional magnetic resonance in this designation will be written in the form R{1,1}, and the EPR found in [10] at the second harmonic and at a threefold field will take the form R{3,2}.

In light of the above, let us consider in more detail the works of the authors [9], [10], where powder samples of DPPH were studied at different frequencies, ac field amplitudes, temperatures, and orientation dependences of the second and third (only in [10]) harmonics of EPR signals. In [9], the experimental results were well described, according to the authors, by formulas obtained on the basis of the theory of quantum mechanics, while in [10] the parameters of the EPR spectra - the arrangement of resonance lines in the field and frequency, in amplitudes and phases - were well described by the modernized Bloch equations [16], [10]. However, a comparative analysis of the results of these works revealed two important and significant differences. Thus, in [10], resonance did not appear at all in a double field, both at the second and third harmonics of EPR signals (multiple frequencies), while in [9] this resonance is seen as intense at a double frequency and a double field (R{2,2}). The opposite picture was observed

with respect to resonance at a threefold field and twofold frequency, i.e. in [10] it is, and in [9] it is absent. An extraordinary situation also developed with the Bloch-Siegert effect (BS) [13], where the authors predicted the absolute shift of the resonance field value as

$$H_{BS1} = -H_1^2/(16H_R). \qquad (1)$$

Here H_1 is the rotating magnetic component from half the amplitude H_p of the plane polarized wave, and H_R is the resonant value of the constant polarizing field. However, in the later works of other authors [14], [17] this shift was defined in the form

$$H_{BS2} = -H_1^2/(4H_R), \qquad (2)$$

It is easy to see that the estimates of shifts in these works differ from the original source [13] by a factor of four. The review article [14, p.474] provides experimental and theoretical arguments confirming the validity of relation (2). This parameter was measured in our work [10] at the second harmonic of the EPR and the result turned out to be suspiciously many times higher than from the most optimistic estimates given in the review [14, p.474]. Such discrepancies in the results required the implementation of further more thorough experimental and theoretical studies.

The aim of this work is to try to find out the reasons for the strong discrepancy between the experimental results and theoretical estimates of different authors on the arrangement of spectral lines, their phases, intensities, shapes, and shifts.

EPR spectrometer for natural experiments

Comparison of experimental installations of these two works showed that Italian physicists [9] used a two-frequency resonator with parallel vibration modes, while in [10] a system of crossed coils (with perpendicular vibration modes) was used. These distinctive features led to different angular dependences of the signals of the second and third harmonics of the EPR. So, in [9], both modes participated in the angular dependence, while in [10] only the receiving coil caused such a dependence, and the transmitting axis always remained orthogonal to the constant field. Since a rather low frequency (11 MHz) and a simplified signal accumulation scheme were used in [10], it became necessary to take measures to increase the signal-to-noise ratio, and also to create conditions for changing the orientation of the constant field to the axis of the transmitting coil, which creates an alternating pump field. For this purpose, the low-frequency EPR spectrometer described in our work [10] was significantly modernized. Thus, the pumping frequency was increased to 20 MHz, the noise parameters of the preamplifier were reduced by 40 MHz, and the digital accumulation (averaging) of the EPR signal spectrum was used. To realize the possibility of changing the angle between the direction of the constant magnetic field

and the axis of the pump coil, an additional magnetizing coil with an axis parallel to the axis of the pump coil is installed, since the mechanical adjustment of this angle was not allowed by the design and dimensions of the Helmholtz coils. The desired angle was set by changing the ratio of the currents (fields) of the Helmholtz coils and this additional coil. A bipolar supply current source was used to neutralize the uncontrolled contributions of external magnetic fields (the Earth's field, for example). The point of transition of a constant field through a zero value was found by the half-sum of resonant fields arising at two inverse currents in the Helmholtz coils. The object of the study was the same powder DPPG that was used in [10]. The functional diagram of the upgraded spectrometer is shown in Fig. 1.
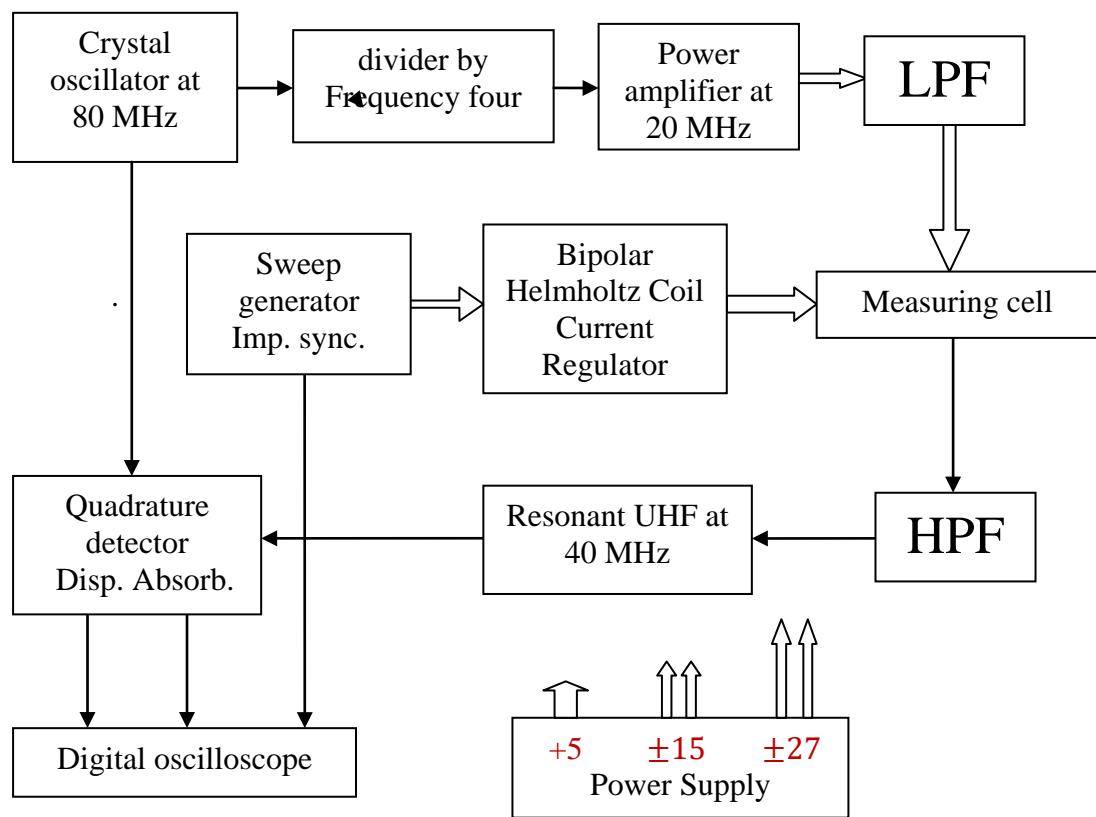
Fig.1 Functional diagram of the EPR spectrometer

As you can see, a master frequency of 80 MHz from a modular crystal oscillator (FT 80.000 MHz) is fed to two trigger dividers (74AC74) from the output of which a 20 MHz signal is fed through a matching transformer to a push-pull adjustable power amplifier up to 10 watts (on two KT904 transistors). A low pass filter (LPF) is used to attenuate possible spurious 40 MHz interference that occurs in the power amplifier. The measuring cell contains two crossed coils - one is a transmitting solenoid, tuned to a frequency of 20 MHz, the other is a two-section receiving saddle, tuned to a signal of the second 40 MHz harmonic of the EPR. Resonant coils

allow working with 10 mm tubes. Helmholtz coils and an additional coil for non-mechanical rotation of the constant field are also located there. Moreover, the axis of this coil is structurally oriented parallel to the axis of the transmitting pump coil. This whole structure is placed in a copper screen with the possibility of forced air ventilation of the Helmholtz coils and the pump coil. Next, the EPR signal is passed through a high-pass filter (HPF), amplified by the input differential stage, and converted by a quadrature detector (AD8348). The components of the absorption and dispersion signals of the EPR from the detector output are recorded by a digital oscilloscope (TDS2012C), usually in the accumulation mode. An analog sweep generator based on the LM2902 microcircuit provides sawtooth signals and pulses for synchronizing the oscilloscope sweep. Its generation frequency can be adjusted within the range of 5-30 hertz. The alternating current stabilizer for Helmholtz coils is assembled on the LM3886 microcircuit and can regulate the current up to ±1 ampere at a load of 20 ohms. The power supply provides voltages: +5 volts for digital microcircuits, ±15 volts for the sweep generator and HF resonant amplifier, and ±27 volts for the HF power amplifier and bipolar current stabilizer. The maximum field strengths oriented along the laboratory axes of coordinates Z and X for a constant field $H_z \cong \pm110$ oersted and the peak value of the variable $H_{px} \cong 7$ oersted, respectively. The maximum value of H_p was achieved when an RF pump power of ~ 10 watts was applied to the resonant LC circuit. The frequency of the constant field sweep H_z was chosen in the range 14–16 hertz.

Computer program for numerical experiments

Even in the very first works of E.K. Zavoisky widely used the terms "perpendicular and parallel fields", meaning the orientation of the variable field $H_p(t) = H_p\cos(\omega_p t)$ to the constant field H_z [18], [19]. He experimentally found out that the perpendicular component $H_{px}(t) = H_p\cos(\omega_p t)$ works in the processes of high-frequency absorption, while the longitudinal component $H_{pz} = H_p(t)\cos(\alpha)$, superimposed on a constant field, creates the effect of modulation of the latter in the form $H_z(t) = H_z + H_{pz}$. Here α is the angle between these fields. These conditions are taken into account in our computer program designed to simulate the EPR spectrum. It is compiled on the basis of MathCAD and is a modernized version of the program used in our work [10]. Below is a screenshot of this program, which solves a system of differential equations (Bloch-2), differentiates, decomposes into a harmonic Fourier series and outputs the calculation results.

$$\gamma := -2 \cdot \pi \cdot 2.804 \quad \omega p := 2 \cdot \pi \cdot f \quad \alpha := \alpha 1 \cdot \pi \cdot 180^{-1} \quad Hpz := Hp \cdot \cos(\alpha) \quad Hpx := Hp \cdot \sin(\alpha)$$

$$Axx := \frac{Hpx^2 \cdot T1^{-1} + 2Hz^2 \cdot T2^{-1}}{Hpx^2 + 2Hz^2} \qquad Ayy := \frac{1}{T2} \qquad Azz := \frac{Hpx^2 \cdot T2^{-1} + 2Hz^2 \cdot T1^{-1}}{Hpx^2 + 2Hz^2}$$

$$Bx := \frac{\chi \cdot Hpx}{T1} \qquad Bz1 := \frac{\chi \cdot Hz}{T1} \qquad Bz2 := \frac{\chi \cdot Hpz}{T1}$$

$$D(t, M) := \begin{bmatrix} -Axx \cdot M_0 + (Hz + Hpz \cdot \cos(\omega p \cdot t)) \cdot \gamma \cdot M_1 + Bx \cdot \cos(\omega p \cdot t) \\ -(Hz + Hpz \cdot \cos(\omega p \cdot t)) \cdot \gamma \cdot M_0 - Ayy \cdot M_1 + Hpx \cdot \gamma \cdot \cos(\omega p \cdot t) \cdot M_2 \\ -Hpx \cdot \gamma \cdot \cos(\omega p \cdot t) \cdot M_1 - Azz \cdot M_2 + Bz1 + Bz2 \cdot \cos(\omega p \cdot t) \end{bmatrix} \qquad \text{(Bloch-2)}$$

$$\Theta := \frac{np2 \cdot tmax^{-1}}{np2 - np1} \qquad\qquad i := 0 .. np2 \qquad Z := \text{rkfixed}(y, 0, tmax, np2, D)$$

$$mx_i := Z_{i,1} \qquad my_i := Z_{i,2} \qquad mz_i := Z_{i,3} \qquad mx_{1202} := 0 \qquad my_{1202} := 0 \qquad mz_{1202} := 0$$

$$nx_i := (mx_{i+1} - mx_i) \cdot \omega p \qquad ny_i := (my_{i+1} - my_i) \cdot \omega p \qquad nz_i := (mz_{i+1} - mz_i) \cdot \omega p$$

$$ReX(n) := \Theta \cdot \sum_{i = np1}^{np2} \left(\cos\left(n \cdot \omega p \cdot \frac{tmax \cdot i}{np2} \right) \cdot nx_i \right) \qquad ImX(n) := \Theta \cdot \sum_{i = np1}^{np2} \left(\sin\left(n \cdot \omega p \cdot \frac{tmax \cdot i}{np2} \right) \cdot nx_i \right)$$

$$ReY(n) := \Theta \cdot \sum_{i = np1}^{np2} \left(\cos\left(n \cdot \omega p \cdot \frac{tmax \cdot i}{np2} \right) \cdot ny_i \right) \qquad ImY(n) := \Theta \cdot \sum_{i = np1}^{np2} \left(\sin\left(n \cdot \omega p \cdot \frac{tmax \cdot i}{np2} \right) \cdot ny_i \right)$$

$$ReZ(n) := \Theta \cdot \sum_{i = np1}^{np2} \left(\cos\left(n \cdot \omega p \cdot \frac{tmax \cdot i}{np2} \right) \cdot nz_i \right) \qquad ImZ(n) := \Theta \cdot \sum_{i = np1}^{np2} \left(\sin\left(n \cdot \omega p \cdot \frac{tmax \cdot i}{np2} \right) \cdot nz_i \right)$$

$$ModX1 := \left(ReX(1)^2 + ImX(1)^2 \right)^{0.5} \qquad\qquad ModY2 := \left(ReY(2)^2 + ImY(2)^2 \right)^{0.5}$$

$$F := (Hz \quad f \quad T1 \quad Hp \quad ModX1 \quad ModY2 \quad ReY(1) \quad ImY(1) \quad ReY(2) \quad ImY(2) \quad ReZ(2) \quad ImZ(2))$$

$$y \equiv (0 \quad 0 \quad 0)^T \qquad\qquad tmax \equiv 1 \qquad np1 \equiv 600 \qquad\qquad np2 \equiv 1200 \qquad\qquad \chi \equiv 0.001$$

$$\text{APPENDPRN}(\text{"N3 (Bloch).dat "}) := F \qquad T1 \equiv 0.06 \qquad T2 \equiv 0.06 \qquad f \equiv 20 \qquad Hp \equiv 1$$

$$F := \text{READPRN}(\text{"N3 (Bloch).dat "}) \qquad \alpha 1 \equiv 67 \qquad Hz2 := (Hz + 0.2) = 14.2 \qquad Hz \equiv 14$$

$$j := 0 .. \text{rows}(F) - 1$$

Fig. 2 Screenshot of a computer program

In this program for a numerical experiment, the EPR spectrum at n-fold frequencies (harmonics) with different signal polarization and slope angle α1 can be obtained by stepwise variation of the constant field Hz or pump frequency f. In the program line F: = (….) 4 set and 8 required parameters are displayed at once. For example, ReY (2) and ImY (2) mean the signals of absorption and dispersion from the receiver coil tuned to the frequency of the second harmonic and the axis parallel to the Y axis. The values of the elements Axx, Azz, Bx and Bz2 of the matrix D (t, M) are taken from [10] with some equivalent mathematical transformations. Elements Axz and Azx are taken equal to zero, since contain the difference between equal relaxation rates 1/T1 and 1/T2. The equality of these times for DPPH is confirmed by experiments [20, p. 393], [21]. It was also found that the original Bloch equations do not describe the case when the constant field is equal to zero [17, p. 55], [22], since they do not take into account the possibility of polarization of the spin system by an alternating field. In the described program, this drawback is eliminated by the fact that it contains the oscillating term Bx * cos (ωt), which appears in the calculations in a natural way, if we consider the development of the original Bloch equations in a swinging coordinate system [10].

Computer processing of EPR spectra

As can be seen from the functional diagram, the spectrometer simultaneously outputs EPR signals in the form of absorption (Abs) and dispersion (Dis) lines. According to the principle of operation of the quadrature detector, the pure shapes of these two components are realized with a sufficiently accurate coincidence of the phases of the reference and received EPR signals. Otherwise, the output of both channels will be a mixture of absorption and dispersion components. Usually, a homogeneous single EPR line from a powder DPPH has a Lorentz shape and can be represented in the form [23], [20, p. 446]:

$$Abs(x) = \frac{Amp * cos(\varphi)}{1+x^2}, \qquad Dis(x) = \frac{Amp * x * sin(\varphi)}{1+x^2} \qquad (3)$$

where φ is the angle between the phases of the reference and received EPR signals,

Amp - EPR signal amplitude,

$x = (H_z\text{-}H_R) / \delta h$ - parameter of detuning of the scanning magnetic field H_z from

the value of the field H_R corresponding to the resonance R{m,n},

δh is the half-width of the resonance line at half the amplitude Amp.

The spectrometer does not have a separate phase φ control. However, it can be changed within small limits by tuning the resonant circuits of the power amplifier and the input amplifier. This phase was selected visually so that the shape of the resonant absorption signal Abs was maximally symmetric. The symmetry of the EPR lines, as shown by the pioneering experiments of E.K. Zavoisky [18], [24], the frequency of EPR detection also affects. Moreover, such a distortion of the resonance line shape turned out to be the greater, the lower this frequency and the wider the resonance line width. This phenomenon can be explained by the effect of not uniform polarization (NUP) of the resonance line across the width during the field scanning, since one half of the line wing is polarized noticeably less than the other half, falling under the conditions of a higher field. This is reflected in the shape of the line, additionally leading to a shift of the extremum of the resonance towards higher fields. It will be shown below that the magnitude of such a shift of the resonance with a positive sign is comparable to the Bloch-Siegert effect. To neutralize the NUP effect when measuring the H_{BS} shift, it turned out to be sufficient to multiply the obtained EPR spectrum data by the correcting normalized factor $\Lambda = H_R/H_z$. Further, to approximate this line, assuming φ = 0, we can use formula (3) with an additional cubic term in the denominator:

$$Abs(H_z) = a + \frac{Amp}{1 + [(H_z - H_{R\pm})/\delta h]^2 + [b(H_z - H_{R\pm})]^3} \qquad (4)$$

The approximation by this function of both experimental (natural) and calculated data Abs_i with the help of an appropriate regression program allows obtaining the most accurate information about the following important parameters, both Amp, δh, and about:

a - displacement of the zero line of the EPR signal,

$H_{R\pm}$- the resonant value of the magnetic field, shifted by the BS and NUP effects,

b - is the asymmetry parameter of the resonant line.

Note that for a single symmetric Lorentzian resonance line, b = 0. In practice, it is enough to reduce this parameter to the value b≤ |0.01| by selecting the phase φ so as to obtain an acceptable measurement accuracy of the shifts H_{BS} and H_{NUP}. After such careful tuning, assuming a = b = 0 and using the Bloch formula [16] [17] for the resonance R{1,1}, the parameters Amp, δh can be expressed in terms of the Bloch times of longitudinal T_1 and transverse relaxation T_2 as:

$$\text{Amp} = Q\omega_p T_2 \chi \gamma H_1 s H_z, \qquad s = [1 + (\gamma H_1)^2 T_1 T_2]^{-1} \quad \text{и} \quad \delta h = \sqrt{(\gamma T_2)^{-2} + H_1{}^2 T_1/T_2}$$

Then formula (4) (for Abs in volts) takes the form

$$Abs(H_z) = \frac{Q\omega_p T_2 \chi \gamma H_1 s H_z}{1 + (H_z - H_{R\pm})^2/[(\gamma T_2)^{-2} + H_1{}^2 T_1/T_2]}, \qquad (5)$$

where:

Q - is a parameter that includes some qualities of the measuring cell and the sample under study, the amplifying and detecting paths of the spectrometer, ω_p- is the pumping frequency, χ - is the paramagnetic susceptibility of the sample, and the γ-gyromagnetic ratio of the electron. Function (5) is interesting in that when the spectrum is taken by scanning the field H_z, its extremum appears not at $H_z = H_R$, but at $H_{R+} > H_R$. The exact value of this field can be found by setting the derivative $d[Abs(H_z)]/dH_z$ to zero. As a result of solving this equation, it is possible to obtain the contribution of the sought-for displacement field due to the NUP

$$H_{R+} = H_R\sqrt{1 + \frac{1}{(T_2\gamma H_R)^2} + \frac{T_1}{T_2}\left(\frac{H_1}{H_R}\right)^2} \cong H_R\left\{1 + \frac{1}{2}\left[\frac{1}{(T_2\gamma H_R)^2} + \frac{T_1}{T_2}\left(\frac{H_1}{H_R}\right)^2\right]\right\}. \quad (6)$$

Let us compare this field with the displaced Bloch-Siegert field with the notation they adopted [13, p. 527]:

$$H_r^* = H_r[1 - H_1^2/(16H_r^{*2})], \quad (7)$$

where under H_r the authors denote the resonant effective field arising when the constant H_z and variable H_1 fields are added, and H_r^* is the observed resonance field shifted downward from H_r. Since the authors renamed H_r^* to H_0 in the annotation, formula (7) can be written:

$$H_{R-} \cong H_0\left[1 - \frac{1}{16}\left(\frac{H_1}{H_0}\right)^2\right]. \quad (8)$$

 As you can see, the corrections to the field in (6) and (8) have opposite signs, and the field H_{R+} depends in a complex way on the mutually orthogonal fields H_z and H_1 and on the relaxation times T_1 and T_2.

Results of natural and numerical experiments

In what follows, in the graphs, the entire spectrum of emerging resonances will be designated, following our work [10], determined by different values **m** (field fold) and **n** (frequency fold) as R{m,n}. The scanning range of the constant field H_z was selected in the range from -25 to +25 oersted. The EPR spectra were obtained at the amplitudes of the alternating field H_p equal to integer values from one to five oersteds. Experimental (natural) results obtained on the spectrometer are shown in Fig. 3 (a, b) and 4 (a, b), and the results of numerical calculations based on the Bloch equations are presented in Fig. 5 (a, b) and 6 (a, b), Measurements were performed at room temperature using a 10 mm glass tube with a powdered DPPG sample. The parameters of the natural and numerical spectra (amplitude, width, BS and NUP shifts were calculated using the method described above.
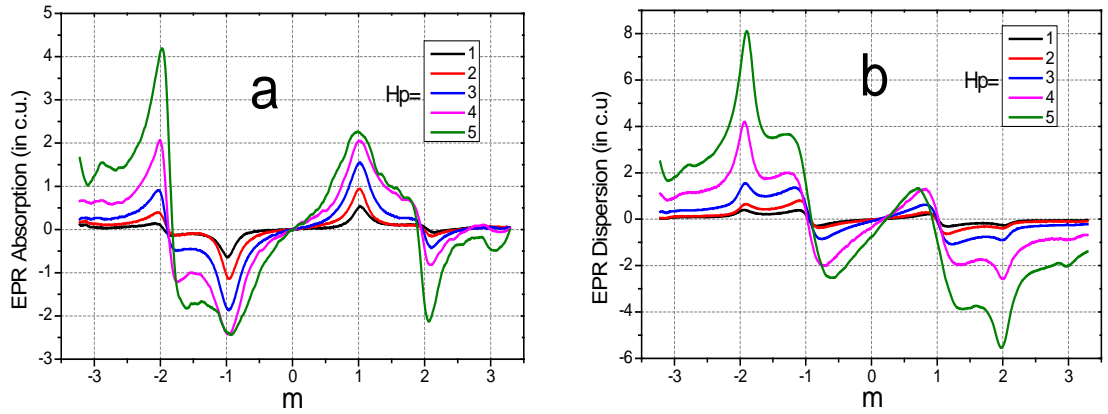
Fig. 3 (a, b) Natural R{m,2} EPR spectra from DPPH (absorption *a* and dispersion *b* in relative units). Cyclic pump frequency ν_p =20 MHz. The axes of the receiving, transmitting and Helmholtz coils are mutually orthogonal (perpendicular fields).
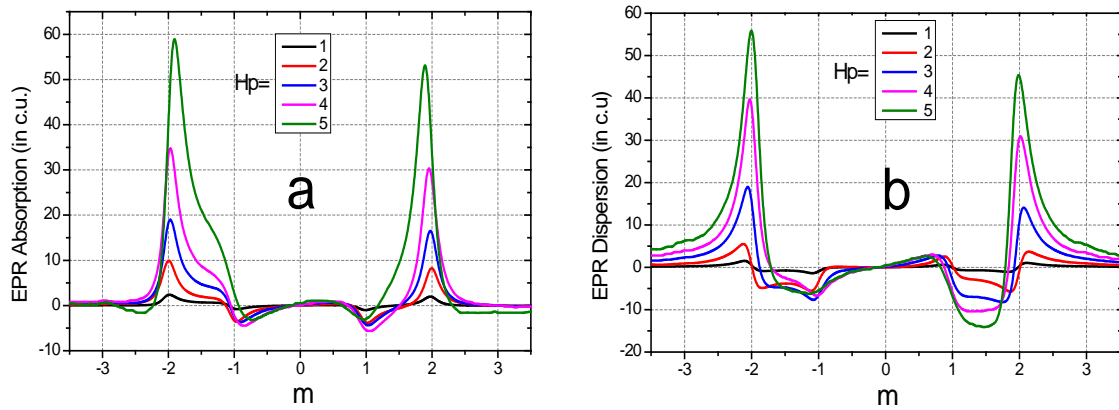

Fig. 4 (a, b) The conditions for obtaining the EPR spectrum are almost the same as in Fig. 2. They differ in that the constant field is inclined to the pump coil axis by 67 degrees, and not 90 degrees as in the previous case. The gain of the receiving path in both Fig. the same.

The results of calculations (numerical experiments) of EPR spectral lines and their main parameters using the above program are shown in Fig. 5, 6, 7, 8, and 9. The paramagnetic susceptibility χ is taken to be 0.001. The quality parameter Q of the receiving path of the spectrometer given in formula (5) by default for all harmonics is taken equal to unity.
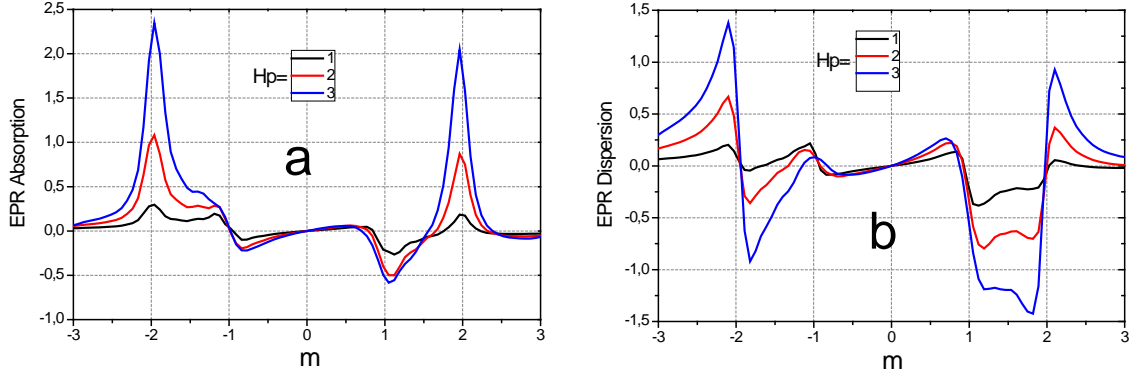
Fig. 5 (a, b) Simulation of the R{m,2} EPR spectra (absorption *a* and dispersion *b* in relative units) were obtained at different specified amplitudes of the alternating magnetic field H_p in steps from one to three oersteds. The pumping frequency and relaxation times are given as $\omega_p = 125.7$ rad/sec and $T_1 = T_2 = 0.06$ sec. accordingly, and the frequency of the receiving section corresponds to the second harmonic of the pump frequency. The axes of the Helmholtz coils, the receiver and the pump are taken to be mutually orthogonal. Since under the experimental conditions in Fig. 3 the computer produces artifacts at the level of calculation error, we had to deviate from strict orthogonality between the axis of the pump coil and the field by only two degrees ($\alpha=88^0$).
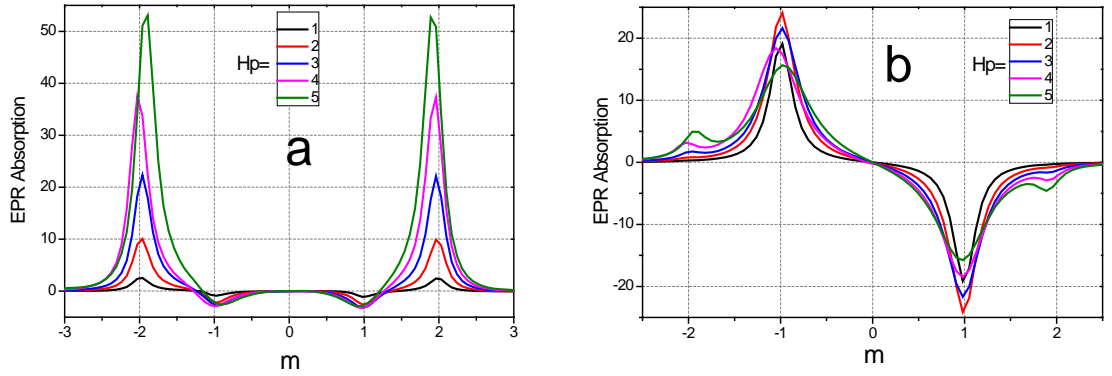

Fig. 6 (a, b). The orientation condition differs from Fig. 5 (a, b) in that the angle of inclination α is chosen equal to 67^0. Fig.6 (a) shows the absorption spectrum R{m,2}, and Fig. 6 (b) - R{m,1}.

EPR line parameters

To obtain more accurate information about the amplitude, width, BS and NUP shifts obtained by natural and numerical experiments, formula (4) was used in the following sequence. For each value of the scanned field H_i with a fixed H_p, the modules were $Mod_i=(Abs_i^2 + Disi2)0,5$ and the angles Ang$i=atan2(Disi/Absi)$.

✓ Using the regression program according to formula (4), the absorption $Abs2_i = Mod_i *$ $\Lambda_i * cos\,(Ang_i + \varphi)$ was found corrected by a fitting angle φ at the minimum b. Here $\Lambda_i = H_R/H_i$ is necessary to neutralize the NUP of the EPR line.

✓ Note that the accuracy and reproducibility of the measured parameters of the resonance line will be the higher, the center of the range of scanned points H_i is close to the value of the resonant field H_R, and the range itself will be within $(2 \div 4)$ δh.

✓ For the same H_p, the data Amp2, the half-width of the line δh2, and the resonance value H_{R-}, containing only the contribution of the shift H_{BS}, were recorded.

✓ The NUP of the line with the same H_p was reconstructed as $Abs3_i = Abs2_i/\Lambda_i$, and again, using the regression program using formula (4), the data for the amplitude Amp3, half-width of the line δh3 and the resonance value $H_{(\pm)}$ containing the total contribution of shifts H_BS and H_NUP. Fig. 7a shows the half-sums of Amp2 and Amp3 as Amp.

✓ The indicated shifts as functions of H_p were calculated by the formulas:

$$H_{BS}\,(H_p) = H_{R-}(H_p) - H_{R-}(H_p = 1), \qquad H_{NUP}\,(H_p) = H_{R\pm}(H_p) - H_{R-}(H_p).$$
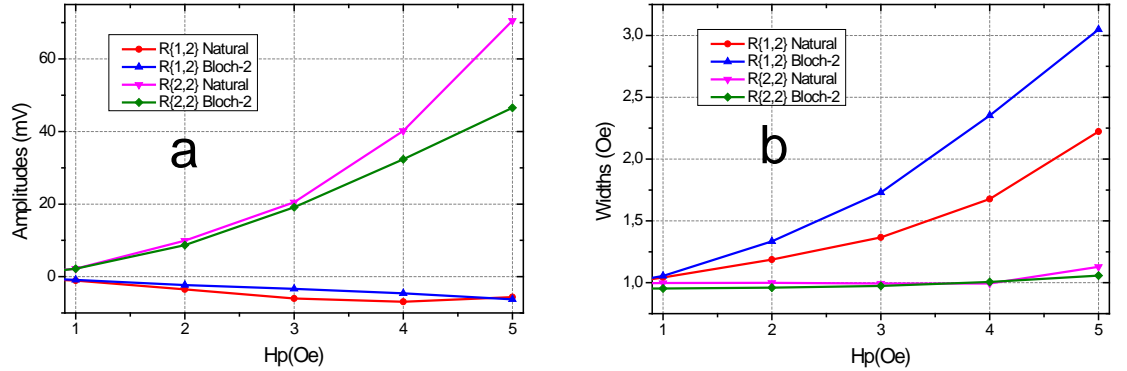

Fig. 7 (a, b) The amplitude Amp and half-width δh of natural (Natural) and numerical (Bloch-2) spectral lines from two types of resonances R{1,2} and R{2,2} depending on the pump amplitude H_p. All results correspond to the orientation $\alpha = 67^0$.
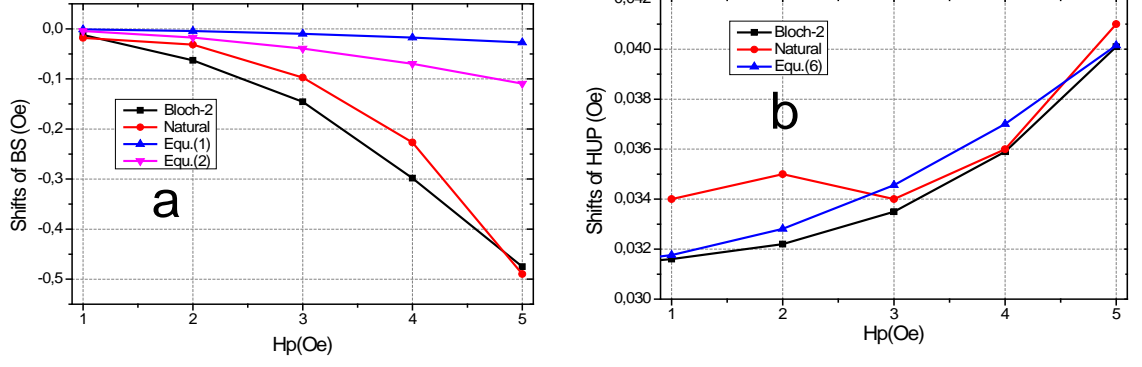
Fig. 8 (a, b). The BS (Bloch-Siegert) and NUP shifts are presented as functions of H_p for the resonance R{2,2}. They were obtained from the data of natural and numerical (Bloch-2) experiments, as well as calculated using formulas (1), (2), and (6) from this article. Here the condition $\alpha = 67^0$ is preserved.
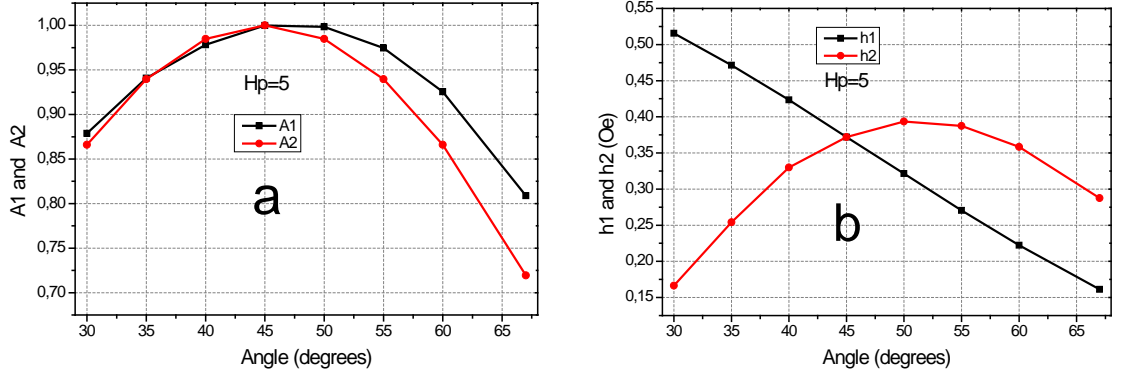

Fig. 9 (a, b). Numerical solutions of Bloch-2 for resonance R{2,2} at Hp = 5 Oe depending on the angle of inclination α (angle). Fig. 9a shows the amplitudes A1=Amp(α)/max (Amp) и A2=sin(2α). According to the graphs in Fig. 9b, for a given angle α, the Bloch-Siegert shift $H_{BS}(\alpha) = h1(\alpha) - 0,644$ can be found, as well as the width of the resonance line $\delta h(\alpha) = 1 + h2(\alpha)/5$.

For a sufficiently correct comparison of the graphs in Fig. 7 (a, b) and Fig. 8 (a, b), the table below shows the relative deviations from each other of the paired data x_i of the natural experiment and the results y_i of numerical calculations in the form of the ratio of the variance σ to the modulus average $\bar{z}$ for all n points of the i-th measurement in percent [25]:

$$\sigma^* = 100\sigma/|\bar{z}| \, , \ \ \sigma = \sqrt{\sum_{i=1}^{n}(x_i - y_i)^2/(n-1)}, \ \ \bar{z} = \sum_{i=1}^{n}(x_i + y_i)/2n.$$

For a more accurate analytical description of the experimental data on the Bloch-Siegert shift, one can use the empirical formula given below. The coefficients of the members of the power series are calculated by the regression program.

$$H_{BS3} = H_p \, (-3,18 + 2,05H_p - 0,67H_p^2) \, / \, 100. \quad\quad (9)$$

This formula was used to calculate the mean square error of the experimental data (variance) $\sigma_{BS3} = 0,0044$ oersted and the modulus of the mean $\bar{z}_{BS3} = 0.172$ oersted.

Table. Comparison of the errors calculated by different formulas for the parameters of the R {2,2} line with respect to the experimental data.

Columns	1	2	3	4	5	6	7	8
Method	Bloch-2	Bloch-2	Equ(6)	Equ(1)	Equ(2)	Bloch-2	Equ(9)
Paramete	Amp	δh	H_{NUP}	H_{NUP}	H_{BS1}	H_{BS2}	H_{BS}	H_{BS3}
$\sigma^* \, (\%)$	50	4,7	5,4	4,8	292	192	34	2,6

Discussion of experimental results and theories

Let us note some interesting features of the results obtained. So, according to the data of a natural experiment in Fig.3 (a, b), inversions of signs and asymmetries of the lines of resonances R{1,2} and R{2,2} are noticeable when the sign of the field H_z changes. There is a noticeable difference in the broadening and the change in their amplitudes with increasing H_p. However, in Fig. 4 (a, b), the picture of resonances changed significantly with the appearance of a slope ($\alpha = 67^0$): the inversion of signs disappeared, but some asymmetry of the line shapes remained. Such trends are qualitatively observed in the results of numerical modeling presented in Fig. 5 (a, b). Fig. 6 (b), the resonance R{2,1} is noticeable at large H_p against the background of the wings R{1,1}, but it disappears if $\alpha = 90^0$. We have no information from the literature on the experimental observation of R{2,1}. According to Fig. 7 (a, b), 8 (a, b), 9 (a, b) and the table above, several interesting features of the resonance R{2,2} can be noted.

➢ This resonance occurs only when there is a longitudinal (modulation) component of the HF pump field ($\alpha \neq 90^0$). Moreover, this condition determines the possibility of the appearance of resonances R{m, n} only with even values of the multiplicity of the fields m.

➢ The resonance R{2,2} undergoes (Fig.7a) insignificant saturation, in contrast to the main (classical) resonance R{1,1} and the resonance R{1,2}.

➢ Its linewidth (δh≅ 1 oersted) almost does not increase (Fig. 7b), while this parameter for other resonances increases several times with an increase in H_p.

➢ The shift H_{BS} (Fig.8a) has a more complex dependence on the value of H_p than the simplified formulas (1), (2) give. Moreover, the results of the numerical solution of the

Bloch equations at least in $\sigma^*(H_{BS2})/\sigma^*(H_{BS}) > 5$ times more accurately describe the natural experiment than the indicated formulas.

➤ The shift H_{NUP} (Fig. 8b), caused by the non-uniformity of polarization (NUP) of the resonance line, varies insignificantly in the range of $0.034 \div 0.041$ oersted. It can be noted that there is a good correlation between the data of natural and numerical methods of experiments, as well as formula (6) with an error of 4.8% (column 6 of the table).

➤ The calculated relative signal amplitude R {2,2} in Fig.9a reaches a maximum, as well as the trial function A2 = Sin (2α), at an angle of inclination $\alpha = 45^0$. With a change in the slope in Fig.9b, both the Bloch-Siegert shift (almost linearly) and the width of the resonance line δh change, reaching a maximum at $\alpha = 50^0$.

On the whole, the EPR model based on Bloch-2 gives a qualitatively satisfactory description of not only four parameters (Amp, δh, H_{NUP}, H_{BS}) of the resonance line R{2,2}, but also the absence or presence of inversion Amp depending on the sign of the field H_z and from the angle of inclination α. Unfortunately, the system of Bloch differential equations without their analytical solution does not allow us to point out the mechanisms of occurrence of certain effects, for example, the metamorphosis of resonances from a change in the sign of the external field H_z at different tilt angles. An attempt to solve them taking into account the new parameters of the matrix Axx, Azz, Bx and Bz2 met with problems. However, a non-rigorous solution can be obtained with some assumptions and reservations if we use the results of work on EPR [19, Chapter 5] and on high-resolution NMR [26, p. 156], [27, p. 273], where the solutions of these equations are given under the joint action on the spin system of perpendicular high-frequency (HF) and parallel low-frequency (LF) fields. In our case, both field components are high-frequency. Therefore, it is possible to admit the applicability of the results of these works for finding an analytical solution of the equations (Bloch-2), if we replace the LF modulation frequency with the HF pump frequency. This replacement made it possible to obtain an approximate analytical solution of these equations. It turned out to be sufficient for a qualitative and visual description of the results of the numerical solution of these equations. We do not present them here, since the calculations and formulas turned out to be very cumbersome and we believe that this topic deserves a separate publication. The solutions obtained show that the intensities of the harmonics numbered n = 0, 1, 2, 3, ... can be found by expanding the function

$$H_s(\alpha, t) = \pm H_z \sqrt{\{1 + kCos(\omega_p t)Cos(\alpha)\}^2 + \{kCos(\omega_p t)Sin(\alpha)\}^2}, \quad k = H_p/H_z, \quad (10)$$

into the trigonometric Fourier series [10]. Note that the intensities of the calculated harmonics are due to the purely nonlinearity of function (10). However, with the interaction of this field with the precessing spin gives rise to the effect modulation of the EPR

frequency, leading to the splitting of each Fourier harmonic into additional symmetric sub harmonics. They are well described by the Bessel functions $J_l(\mu_n)$ of the first kind of the l-th order of the actual individual argument (modulation index) μ_n for each harmonic $\boldsymbol{n\omega_p}$ [29, p.418]. It turns out that the inversion of the EPR sign or its absence when the polarity H_z changes is due to the odd property of the first-order Bessel function with the modulation index for the second harmonic - $J_1(\mu_2)$. So, in the case of resonance R{2,2}, the dependences of Amp and δh on the angle α and on the amplitude H_p are also described quite correctly by the functions $J_0(\mu_2)$ and $J_1(\mu_2)$. As for the Bloch-Siegert shift, it is determined by the modulation index of the zero harmonic μ_0 {$Cos(n\omega_p t) = 1$, for n = 0}.

Thus, the theoretical model we used by F. Bloch (Bloch-2) describes quite correctly a number of important physical parameters of EPR lines not only in perpendicular fields (R{1,2}, R{1,3}, R{3,2} and R{3,3}; [10]), but also on oblique ones (R{1,1}, R{2,1} and R{2,2}; $\alpha \neq 90^0$). However, the percentages of significant discrepancy between the Bloch-2 data and the experiment for Amp (50%) and H_{BS} (34%) cannot be attributed to the errors of the equipment and methods of EPR data processing, since the error of our spectrometer does not exceed 2.6%. In our opinion, there are several reasons for this.

First, the Bloch equations do not take into account dipole-dipole interactions, although these effects are indirectly manifested at the values of T_2. In reality, a purely quantum effect is reflected on T_2, which is called in the literature the exchange narrowing of the resonance line [3, Ch. IV], [28], which is also not taken into account in the Bloch model.

Second, the possible influence of high-power high-frequency pumping on the g-factor of an electron is also ignored. Such a metamorphosis of the g-factor was observed on Mn^{2+} ions at low EPR observation fields [3, p. 19].

Third, it is impossible in numerical calculations to separate the contribution of the neighboring resonance, for example, the high-field wing R{1,2} into the shape and center R{2,2}, which can give an additional error in the measurement of the Bloch-Siegert shift. A more correct analytical solution of the Bloch system of differential equations would allow to eliminate this error.

The indicated drawbacks cannot diminish the obvious and considerable advantages of the Bloch equations described above and deserve further modernization, taking into account multiquantum and multiphoton effects.

It should be noted that the EPR spectrometer at low frequencies with a "non-traditional orientation" between constant and alternating fields and with multiphoton frequency multiplication has been very successful in studying the Bloch-Siegert effect. This became

possible due to the fact that the absolute shift BS is the greater, the smaller the field H_z (see formulas (1) and (2)), due to which we managed to work with a more accessible object of study (DPPH). For comparison, in [30], in order to overcome this undesirable effect arising in an EPR spectrometer in the centimeter range, they had to use unique, difficult to prepare samples with record narrow EPR lines.

Conclusion

Novelty. Based on the obtained experimental EPR spectra and calculated using the data of the modernized equations:

❖ discovered (quite by accident) the effect of inversion and asymmetry of EPR lines on harmonics when the constant field sign changes and a variant of the explanation of this effect is given;

❖ the conditions for maximizing the signal of the second harmonic of the EPR are shown depending on the angle of inclination of the HF field to the constant field;

❖ a technique for a more correct measurement of the Bloch-Siegert shift with the subtraction of the EPR line shift caused by the polarization non uniformity (NUP) of these lines during scanning of a constant field has been proposed;

❖ it is shown that the experimentally measured parameters of resonance lines, such as their amplitude, width, shape, Bloch-Siegert shift and the effect of the appearance of observed and possible resonant EPR harmonics, are well described by the modernized Bloch equations. Moreover, these equations describe the Bloch-Siegert shift according to the data of a natural experiment many times more accurately than the estimates of the theories known to us.

Perspective. Based on the above material, one can expect the creation of (exclusive, small-scale) EPR spectrometers based on harmonics with tilted single- and multimode resonators with high pump field levels without any particular fear of saturation and broadening of the spectral lines of the resonance R{2,2}. Such devices can occupy an intermediate niche between pulsed and continuous mode spectrometers operating at the fundamental (Larmor) EPR frequency and can be competitive in the study of both narrow and wide EPR lines. The described effect of harmonic generation can be useful in the field of NMR, for example, in geological devices using the Earth's magnetic field [31], in devices for the needs of the oil industry [32], [33].

spectrometer, as well as to the director of the Museum-Laboratory named after E.K. Zavoisky [34] - Silkin I.I. for very interesting and useful advice.

Literature

1. N. B. Delone. Multi-quantum processes. "Quant", No. 5, pp. 23-29 (1989).

2. P. P. Sorokin, I. L. Gelles, and W. V. Smith. Multi-photon Rabi oscillations in high spin paramagnetic impurity, Phys. Rev. Vol. 112, Num. 5, pp. 1513-1515, (1958).

3. S.A. Altshuler, B.M. Kozyrev. Electronic paramagnetic resonance of compounds of elements of intermediate groups. - M .: Science, (1972).

4. E.K. Zavoisky. Determination of magnetic and mechanical moments of atoms in solids. DAN SSSR, 57, 887, (1947).

5. A. Abraham, B. Blini. Electronic paramagnetic resonance of transition ions. "MIR", Moscow, (1972).

6. N. Noginova, T. Weaver, E. P. Giannelis, A. B. Bourlinos, V. A. Atsarkin, and V. V. Demidov. OF OBSERVATION MULTIPLE QUANTUM TRANSITIONS IN MAGNETIC NANOPARTICLES. Phys. Rev. B 77, 014403 - Published 3 January (2008).

7. N. Noginova, Yu. Barnakova, A. Radocea, V.A. Atsarkin. Role of dipole – dipole interactions in half-field quantum transitions in magnetic nanoparticles. Journal of Magnetism and Magnetic Materials. Vol. 323, Issue 17, Pages 2264-2270, (2011)

8. N.B. Delone. Multiphoton processes. Soros Educational Journal, No. 3, (1996).

9. R. Boscaino, I. Ciccarello, C. Cusumano, and M. W. P. Strandberg, Second-Harmonic Generation and Spin Decoupling in Resonant Two-Level Spin Systems, Phys. Rev. B, Vol. 3 Num 3 (1971).

10. I.I. Sadykov. The role of the parameters of the fields of external action on the spin-system in the processes of generation of harmonics. Letters to ZhETF, vol. 66, no. 2, pp. 104-109 (1997).

11. Moritz Kälin, Matvey Fedin, Igor Gromov and Arthur Schweiger. Lect. Notes, Multiple-photon transitions in EPR spectroscopy, Phys. 684, 143-183 (2006).

12. Moritz Kälin. Multiple Photon Processes in Electron Paramagnetic Resonance Spectroscopy. Dissertation (2003).
https://link.springer.com/chapter/10.1007%2F3-540-32627-8_6

13. F. Bloch and A. Siegert, Magnetic resonance for nonrotating fields, Phys. Rev. 57, 522 (1940).

14. L.N. Novikov, G.V. Skrotsky. Nonlinear and parametric effects in atomic radiospectroscopy Phys. Uspekhi, vol. 125, no. 3 (1978).

15. V.A. Morozov. Development of the theory of multi-quantum, relaxation and magneto-structural transitions in spin systems. Doct. Diss., Novosibirsk (2011).

16. F. Bloch. Nuclear Induction. Phys. Rev. Vol. 70, no. 7 and 8, (1946).

17. A. Abragam, The principles of nuclear magnetism, Oxford (1961).
    (A. Abraham, Nuclear Magnetism, Moscow (1963)).

18. E.K. Zavoisky, Paramagnetic absorption in perpendicular and parallel fields for some salts, solutions and metals. Dissertation, FIAN, Moscow (1944).

19. E.K. Zavoisky, Measurement of the magnetic susceptibility of paramagnets at decimeter waves. ZhETV, 17, 155 (1947).

20. Ch. Poole. EPR spectroscopy technique. "WORLD" (1970).

21. J.P. Lloyd, G.E. Pake, Spin-lattice relaxation and the residual width of highly exchange-narrowed paramagnetic resonances, Phys. Rev. 92, 1576 (1953).

22. G. Whitfield, A. G. Redfield, Paramagnetic resonance detection along the polarizing field direction. Phys. Rev. 106, 918 (1957).

23. G. E. Pake, E. M. Pursell, Line shapes in nuclear paramagnetism.
    Phys. Rev. 74, 1184 (1948).

24. E.K. Zavoisky. Magnetospin resonance in the region of decimeter waves. J. Phys. USSR, 10, 197 (1946).

25. Yu.A. Kravtsov, Randomness, Determination, Predictability. UFN, Volume 158, no. 1, 93 (1989).

26. V. Anderson. Magnetic field modulation in high-resolution NMR spectrometers. (In the book NMR and EPR spectroscopy, on page 156, MIR, Moscow (1964).

27. J. Peik. Fundamentals of the theory of nuclear magnetic resonance. (In the book "NMR - and EPR spectroscopy", on p. 153, "MIR", Moscow (1964).

28. KM Salikhov, State of the theory of spin exchange in dilute solutions of paramagnetic particles. A new paradigm of spin exchange and its manifestations in EPR spectroscopy, UFN, 189, No. 10 (2019).

29. André Ango, Mathematics for Electrical and Radio Engineers. "Science", Moscow (1964).

30. A.P. Saiko, G.G. Fedoruk. Influence of the Bloch-Siegert shift on the amplitude-frequency characteristics of Rabi oscillations at nutational resonance, Letters to ZhETF, vol. 87, no. 3, p. 154-158 (2008).

31. N.M. Pomerantsev, V.M. Ryzhkov, G.V. Skrotsky, Physical Foundations of Quantum Magnetometry, Moscow, "Science" (1972)

32. V. Odivanov, R. Kurbanov, I. Sadykov, A. Kharisov. Hardware and software complex "Kanal Kvant" for measuring the composition and flow rate of fluid produced from oil wells, CTA, No. 2, pp. 44-48 (2006). www.cta.ru

33. V. Ya. Volkov, B.V. Sakharov, N.M. Khasanova, D.K. Nurgaliev. Analysis of the compositional composition and properties of heavy oils in situ by NMR relaxation in low magnetic fields. Georesources, 20 (4), Part 1, p. 308-323, (2018).

34. Museum, https://kpfu.ru/museums/muzej-laboratoriya-ekzavojskogo